Multistage genome-wide association meta-analyses identified two new loci for bone mineral density

Lei Zhang[1,2], Hyung Jin Choi[4,†], Karol Estrada[5,6,7,†], Paul J. Leo[8,†], Jian Li[2], Yu-Fang Pei[1,2], Yinping Zhang[2], Yong Lin[1], Hui Shen[2], Yao-Zhong Liu[2], Yongjun Liu[2], Yingchun Zhao[2], Ji-Gang Zhang[2], Qing Tian[2], Yu-ping Wang[2], Yingying Han[1], Shu Ran[1], Rong Hai[1], Xue-Zhen Zhu[1], Shuyan Wu[1], Han Yan[2], Xiaogang Liu[2], Tie-Lin Yang[2], Yan Guo[2], Feng Zhang[2], Yan-fang Guo[2], Yuan Chen[2], Xiangding Chen[2], Lijun Tan[2], Lishu Zhang[2], Fei-Yan Deng[2], Hongyi Deng[2], Fernando Rivadeneira[5,6,7], Emma L Duncan[8,9], Jong Young Lee[10], Bok Ghee Han[10], Nam H. Cho[11], Geoffrey C. Nicholson[12], Eugene McCloskey[13,14], Richard Eastell[13], Richard L. Prince[15,16], John A. Eisman[17], Graeme Jones[18], Ian R. Reid[19], Philip N. Sambrook[20], Elaine M. Dennison[21], Patrick Danoy[8], Laura M. Yerges-Armstrong[22], Elizabeth A. Streeten[22,23], Tian Hu[3], Shuanglin Xiang[24], Christopher J. Papasian[25], Matthew A. Brown[8,†], Chan Soo Shin[4,†], André G. Uitterlinden[5,6,7,†] and Hong-Wen Deng[1,2,*]

[1]Center of System Biomedical Sciences, University of Shanghai for Science and Technology, Shanghai, China, [2]Department of Biostatistics and Bioinformatics and [3]Department of Epidemiology, Tulane University, New Orleans, LA, USA, [4]Department of Internal Medicine, Seoul National University College of Medicine, Seoul, Korea, [5]Department of Internal Medicine and [6]Department of Epidemiology, Erasmus Medical Center, Rotterdam, The Netherlands, [7]Netherlands Genomics Initiative (NGI)−Sponsored Netherlands Consortium for Healthy Aging (NCHA), Leiden, The Netherlands, [8]Human Genetics Group, University of Queensland Diamantina Institute, Brisbane, Queensland, Australia, [9]Department of Endocrinology, Royal Brisbane and Women's Hospital, Brisbane, Queensland, Australia, [10]Center for Genome Science, National Institute of Health, Osong Health Technology Administration Complex, Chungcheongbuk-do, Korea, [11]Department of Preventive Medicine, Ajou University School of Medicine, Youngtong-Gu, Suwon, Korea, [12]Rural Clinical School, The University of Queensland, Toowoomba, Australia, [13]Academic Unit of Bone Metabolism, Metabolic Bone Centre, University of Sheffield, Sheffield, UK, [14]NIHR Musculoskeletal Biomedical Research Unit, Sheffield Teaching Hospitals Trust, Sheffield, UK, [15]School of Medicine and Pharmacology, University of Western Australia, Perth, Australia, [16]Department of Endocrinology and Diabetes, Sir Charles Gairdner Hospital, Perth, Australia, [17]Garvan Institute of Medical Research, University of New South Wales, Sydney, Australia, [18]Menzies Research Institute, University of Tasmania, Hobart, Australia, [19]Department of Medicine, University of Auckland, Auckland, New Zealand, [20]Kolling Institute, Royal North Shore Hospital, University of Sydney, Sydney, Australia, [21]Medical Research Council Lifecourse Epidemiology Unit, University of Southampton, Southampton, UK, [22]Program in Personalized and Genomic Medicine, and Department of Medicine, Division of Endocrinology, Diabetes and Nutrition, University of Maryland School of Medicine, Baltimore, MD, USA, [23]Geriatric Research and Education Clinical Center (GRECC), Veterans Administration Medical Center, Baltimore, MD, USA, [24]Key Laboratory of Protein Chemistry and Developmental Biology of State Education Ministry of China, Hunan Normal University, Changsha, China and [25]Department of Basic Medical Science, University of Missouri-Kansas City, Kansas City, MO, USA

*To whom correspondence should be addressed at: Center for Bioinformatics and Genomics, School of Public Health and Tropical Medicine, Tulane University, 1440 Canal Street, Suite 2001, New Orleans, LA 70112, USA. Tel: +1 5049881310. Email: hdeng2@tulane.edu
†These authors contributed equally to this work. Their orders of appearances are arranged in alphabetical order of their last names.

Aiming to identify novel genetic variants and to confirm previously identified genetic variants associated with bone mineral density (BMD), we conducted a three-stage genome-wide association (GWA) meta-analysis in 27 061 study subjects. Stage 1 meta-analyzed seven GWA samples and 11 140 subjects for BMDs at the lumbar spine, hip and femoral neck, followed by a Stage 2 *in silico* replication of 33 SNPs in 9258 subjects, and by a Stage 3 *de novo* validation of three SNPs in 6663 subjects. Combining evidence from all the stages, we have identified two novel loci that have not been reported previously at the genome-wide significance (GWS; 5.0×10^{-8}) level: 14q24.2 (*rs227425*, *P*-value 3.98×10^{-13}, *SMOC1*) in the combined sample of males and females and 21q22.13 (*rs170183*, *P*-value 4.15×10^{-9}, *CLDN14*) in the female-specific sample. The two newly identified SNPs were also significant in the GEnetic Factors for OSteoporosis consortium (GEFOS, *n* = 32 960) summary results. We have also independently confirmed 13 previously reported loci at the GWS level: 1p36.12 (*ZBTB40*), 1p31.3 (*GPR177*), 4p16.3 (*FGFRL1*), 4q22.1 (*MEPE*), 5q14.3 (*MEF2C*), 6q25.1 (*C6orf97*, *ESR1*), 7q21.3 (*FLJ42280*, *SHFM1*), 7q31.31 (*FAM3C*, *WNT16*), 8q24.12 (*TNFRSF11B*), 11p15.3 (*SOX6*), 11q13.4 (*LRP5*), 13q14.11 (*AKAP11*) and 16q24 (*FOXL1*). Gene expression analysis in osteogenic cells implied potential functional association of the two candidate genes (*SMOC1* and *CLDN14*) in bone metabolism. Our findings independently confirm previously identified biological pathways underlying bone metabolism and contribute to the discovery of novel pathways, thus providing valuable insights into the intervention and treatment of osteoporosis.

INTRODUCTION

Osteoporosis is the most common metabolic skeletal disorder in humans. It predisposes people to fragility fracture particularly at the hip and confers substantial morbidity and mortality (1), affecting over 200 million people worldwide (2).

Osteoporosis is mainly characterized by low bone mineral density (BMD), which is highly heritable with heritability ranging from 0.5 to 0.8 (3). To date, genome-wide association studies (GWASs) and their meta-analyses have identified over 50 loci associated with variations in BMD (4–12). Cumulatively, however, genetic loci identified through GWAS account for no more than 6% of total BMD phenotypic variation (6). Therefore, there is little doubt that additional novel loci await to be uncovered. We here report a new multistage genome-wide association meta-analysis of samples of diverse ancestries and of imputed sequence variants with the 1000 genomes project (1KG) reference panels (13).

RESULTS

This study of meta-analysis comprises three stages (Fig. 1). Stage 1 incorporated seven GWAS samples encompassing 11 140 individuals of diverse ancestries (Supplementary Material, Table S1). The majority (7738; 69.5%) of the individuals were women. Principal component analysis (PCA) was applied to each individual sample (14), and no population outliers were observed. Imputation with the 1KG reference panels generated 5 842 825 SNPs that were qualified for analysis (Supplementary Material, Table S2). After adjusting phenotypes by PCA in each individual study (14), overall genomic control inflation factors were small or modest in both individual GWAS and meta-analysis for each of the spine (SPN-), total hip (HIP-) and femoral neck (FNK-) BMD traits ($\lambda = 0.99–1.06$, Supplementary Material, Table S2), implying the limited effects of potential population stratification. A logarithmic quantile–quantile plot of the meta-analysis test statistics showed a marked deviation in the tail of the distribution, both in the gender combined and female-specific samples, implying the possible existence of true associations in these samples (Fig. 2). In the combined sample, a total of 281 SNPs from 10 genomic loci were associated with BMD at the genome-wide significance (GWS; 5.0×10^{-8}) level (Supplementary Material, Table S3). Another 102 SNPs from 18 additional loci yielded *P*-values between 1.0×10^{-6} and 5.0×10^{-8}, which was defined as a borderline association (Supplementary Material, Table S4). In the female-specific sample, 45 SNPs from four loci were associated with BMD at the GWS level (Supplementary Material, Table S3); all of these loci overlapped with those identified with the combined sample. Another seven SNPs from an additional four loci were associated at the borderline level (Supplementary Material, Table S4). In the male-specific sample, only one SNP (*rs77687936* in 9q21.33) was associated with HIP-BMD at the borderline level ($P = 1.88 \times 10^{-7}$, Supplementary Material, Table S4). In total, 303 SNPs from 10 different genomic regions were associated with BMD at the GWS level, and 138 from an additional 23 regions fell into the borderline level.

To validate the findings of Stage 1, one SNP (generally the one with the strongest signal, with a few exceptions in which the consistency of effect directions was also considered) from each of the 33 (10 GWS plus 23 borderline) regions was selected and subjected to Stage 2 *in silico* analysis in another three independent GWAS samples encompassing 9258 individuals (Supplementary Material, Tables S1 and S5). In the joint analyses of Stages 1 and 2, 9 of the 10 SNPs attaining GWS level in Stage 1 retained significance at the GWS level, whereas the last SNP *rs11696050* was filtered out. Of the 23 borderline SNPs, the signals at five SNPs (*rs525592*, *rs6827815*, *rs9533095*, *rs1463104* and *rs227425*) emerged as being significant at the GWS level, and that of *rs170183* nearly reached the GWS level in the female-specific sample ($P = 6.16 \times 10^{-8}$). No significant, or nearly significant, associations were identified in the male-specific samples. In total, 15 SNPs were identified as being significant, or nearly significant (*rs170183*), at the GWS level by the joint analysis of Stages 1 and 2.

Twelve of these 15 SNPs reside in genomic regions that had previously been reported to be associated with variations in

BMD at the GWS level (4,7,8,11). Of the remaining three SNPs, two reside in genomic regions 14q24.2 (*rs227425*) and 21q22.13 (*rs170183*), respectively, which had not been previously reported at the GWS level; the third SNP, *rs6827815,* resides in 4p16.3 which was independently reported by the GEnetic Factors for osteoporosis consortium (GEFOS) during the preparation of this manuscript (6). To validate these three SNPs (*rs227425*, *rs170183* and *rs6827815*), they were *de novo* genotyped in a Stage 3 replication study of two additional independent samples encompassing 6663 subjects of European- and East Asian-ancestries. All the three SNPs showed evidence of

association after Bonferroni correction of multiple testing (0.05/3 ≈ 0.02) in the Stage 3 meta-analysis, though *rs170183* did not reach the nominal level in Asian subjects (Supplementary Material, Table S6). They remained to be significant at the GWS level in the joint analyses of the three stages (Tables 1 and 2).

During preparation of this manuscript, the GEFOS released genome-wide association summary results in samples of as many as 17 discovery GWAS samples and 32 960 subjects (6). We checked the replicability of the two newly identified SNPs (*rs227425* and *rs170183*) in the GEFOS results. Two samples (FHS and IFS) in Stage 1 and two in Stage 2 [Rotterdam study (RS) and AOGC] of the present study overlapped with the GEFOS samples; therefore, the GEFOS summary results could not be readily used as independent replication. We were able to obtain replication data of three of the GEFOS remaining samples: two ($n = 1479$ and 2762, respectively) from the TwinsUK cohort and the third from the Amish family osteoporosis study (AFOS, $n = 918$). The results were listed in Supplementary Material, Table S7. One of the TwinsUK samples successfully replicated *rs227425* ($P = 0.02$) at 0.05 level. Both TwinsUK samples replicated the effect direction of *rs170183*, though neither *P*-value was significant. The AFOS sample (475/918 female/combined subjects) replicated neither *P*-value nor direction at both SNPs, likely due to the relatively small sample size, among other things. To incorporate the entire GEFOS results, we performed two alternative analyses. In the first analysis, we analyzed associations in the GEFOS remaining samples. In the second analysis, we analyzed associations in the remaining samples of the present study, and then integrated the GEFOS summary results as a whole. For the first analysis, though association signals at the GEFOS remaining non-overlapped samples were not publicly available, we could derive them analytically given signals at combined samples (overlapped plus remaining) and at overlapped samples (Supplementary Material). In Supplementary Material, Table S8, we derived the *P*-values at *rs227425* and *rs170183* were 0.18 and 1.41×10^{-3} in the GEFOS remaining samples, respectively, both having the same effect direction as that in the present study. In this sense, *rs170183* was successfully replicated by the GEFOS remaining samples. Though *rs227425* was not
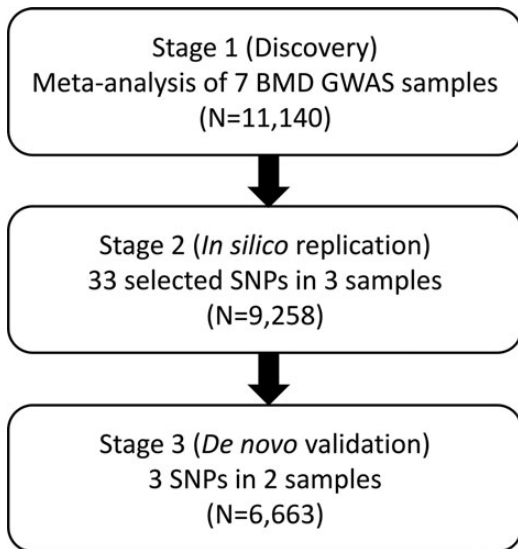

Figure 1. Diagram workflow of the study design. This study of meta-analysis comprises three stages. In the first stage, seven genome-wide association study (GWAS) samples were analyzed for a meta-analysis. In the second stage, a set of significant SNPs were selected from Stage 1 and subjected to *in silico* analysis in three additional samples. Novel SNPs significant (or nearly significant) at the GWS level from joint analysis of the above stages were followed up by Stage 3 *de novo* genotyping in two additional samples. BMD: bone mineral density.
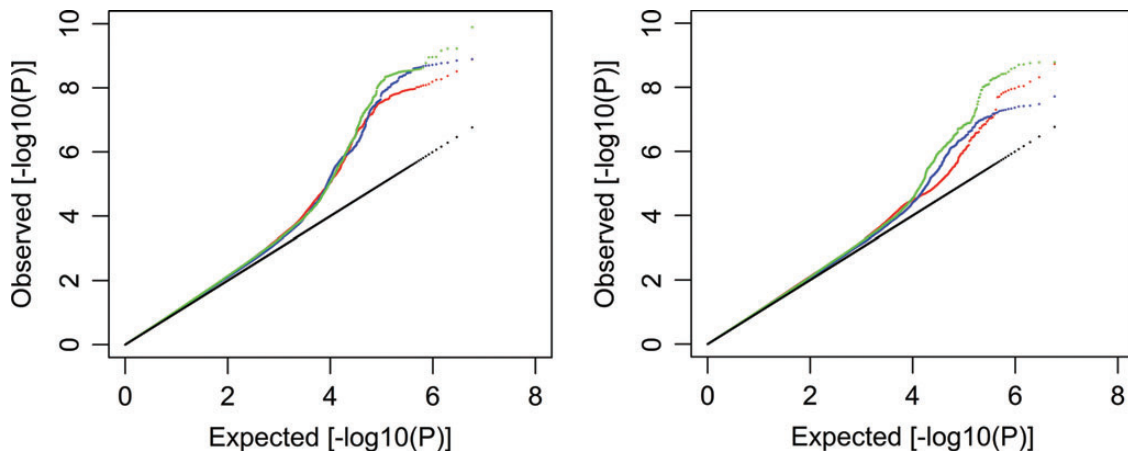

Figure 2. Stage 1 logarithmic quantile–quantile (QQ) plot of GWAS results. A logarithmic QQ plots for BMDs in the combined sample (left) and in the female-specific sample (right). For each sample, results were plotted for the hip (red), femoral neck (blue) and spine (green) BMDs.

Table 1. New SNPs identified at the GWS level

Locus	SNP	Alleles	Freq	Gene	Sample	Stage	Sample size	HIP				FNK				SPN			
								Beta	Fixed	Random	I^2	Beta	Fixed	Random	I^2	Beta	Fixed	Random	I^2
14q24.2	*rs227425*	G/T	EUR:0.53 ASI:0.48 AFR:0.70	*SMOC1*	Combined	1	10 917	−1.33	8.32E−4	3.15E−3	29.1	−0.84	0.04	0.11	47.5	−2.05	2.69E−7	2.69E−7	0.0
						2	8469	−0.79	0.26	0.26	0.0	−0.81	0.25	0.40	40.4	−2.09	5.16E−4	0.03	0.0
						1 + 2	19 386	−1.19	6.35E−4	1.39E−3	20.4	−0.81	0.02	0.06	39.1	−2.06	**7.41E−10**	**2.20E−9**	0.0
						3	6663	−2.44	5.98E−4	0.13	85.0	−2.37	8.54E−4	0.03	70.6	−2.73	1.20E−4	1.20E−4	19.4
						1 + 2 + 3	26 049	−1.50	2.03E−6	3.24E−4	43.1	−1.19	1.63E−4	5.37E−3	46.8	−2.20	**3.98E−13**	**8.30E−13**	0.0
21q22.13	*rs170183*	G/A	EUR:0.53 ASI:0.41 AFR:0.13	*CLDN14*	Female	1	7360	1.99	3.71E−7	1.13E−5	0.0	1.81	4.44E−6	4.44E−6	0.0	1.50	3.25E−4	3.25E−4	0.0
						2	1399	1.89	0.06	0.06	0.0	1.32	0.07	0.07	22.4	2.09	0.04	0.04	0.0
						1 + 2	8759	1.98	6.16E−8	4.44E−7	0.0	1.67	1.70E−6	1.70E−6	0.0	1.51	3.66E−5	3.66E−5	0.0
						3	3841	1.76	0.01	0.01	0.0	1.81	0.01	0.01	0.0	1.20	0.09	0.09	0.0
						1 + 2 + 3	12 600	1.92	**4.15E−9**	**4.15E−9**	0.0	1.70	5.88E−8	5.88E−8	0.0	1.43	1.17E−5	1.17E−5	0.0

We used METAL (15) to perform fixed-effects meta-analysis, which performed on normally transformed quantiles from individual study *P*-values, and weighted by square root of sample size. Random-effects meta-analysis was performed with the procedure *meta.summaries* within the R package *rmeta*. Beta: regression coefficient for transformed quantiles on the first allele (**G**); Fixed: fixed-effects model *P*-value; Random: random-effects model *P*-value; I^2: heterogeneity measure; HIP: hip BMD; FNK: femoral neck BMD; SPN: spine BMD; EUR: European; ASI: Asian; AFR: African. *P*-values of genome-wide significance were marked in bold.

replicated at $P = 0.05$, its effect direction was indeed consistent. For the second analysis, after removing four overlapped samples (FHS, $n = 3747$; IFS, $n = 1488$; RS, $n = 4904$; AOGC, $n = 1955$; total $n = 12\ 094$) from the present study, *P*-values at *rs227425* and *rs170183* were 1.34×10^{-10} and 3.74×10^{-6} (Supplementary Material, Table S9). *P*-values in the GEFOS samples were 1.24×10^{-3} and 5.90×10^{-4}. Therefore, both SNPs were successfully replicated by the GEFOS. Though *rs170183* was not significant at the GWS level in the present study without the four overlapped samples, including the GEFOS signal (with all the GEFOS samples) did reached a GWS signal ($P = 4.62 \times 10^{-8}$).

For the two familial samples (FHS and IFS), we used the method that we developed previously to test association (16). Here, we verified the analyses by two alternative methods. The first method was Chen and Abecasis (17), which gave nearly identical *P*-values to our previous analyses (Supplementary Material, Table S10). The second method was the transition disequilibrium test (TDT) implemented in PLINK (18). Signals at both SNPs by TDT got weaker (Supplementary Material, Table S10), implying that TDT was possibly low-powered, as is generally expected (16,17).

rs227425 was associated with SPN-BMD at the GWS level ($P = 3.98 \times 10^{-13}$, Table 1); the associations for both HIP-BMD ($P = 2.03 \times 10^{-6}$) and FNK-BMD ($P = 1.63 \times 10^{-4}$) were also suggestively significant. Allele G at this imputed SNP has a frequency between 0.48 (East Asian) and 0.70 (African) and tended to decrease BMDs (Fig. 3). This SNP is located in an intron of the *SMOC1* (secreted modular calcium-binding protein 1) gene (Supplementary Material, Fig. S1) in 14q24.2. Though several other genes, including *SRSF5*, *SLC10A1* and *SLC8A3*, also reside in this region, *SMOC1* is of particular interest because of its known regulatory function on bone development. This gene encodes a glycoprotein with a calcium-dependent conformation (19). It acts as a regulator of osteoblast differentiation of bone marrow-derived mesenchymal stem cells (20), and is essential for ocular and limb development (21). Its regulatory mechanism also involves antagonism of activities of bone morphogenetic protein (18).

The association of the imputed SNP *rs170183* in 21q22.13 was only found in the female-specific sample, most convincingly with HIP-BMD ($P = 4.15 \times 10^{-9}$, Tables 1), but also with FNK-BMD ($P = 5.88 \times 10^{-8}$) and SPN-BMD ($P = 1.17 \times 10^{-5}$). There was no evidence of association in the male-specific sample (HIP-BMD $P = 0.26$). Allele G at this SNP increased BMD (Fig. 3). This region has been previously reported to be associated with hip ($P = 3.90 \times 10^{-4}$) and spine ($P = 7.70 \times 10^{-3}$) BMDs in a female-specific sample through two SNPs (*rs219779* and *rs219780*), though neither of the signals achieved GWS in that study (22). In the present study, the signals at both SNPs were weak (*rs219779* $P = 0.04$; *rs219780* $P = 0.07$, for HIP-BMD). Though the two SNPs were in strong LD with each other ($r^2 = 0.75$), neither of them was strongly correlated with *rs170183* (*rs219779* $r^2 = 0.24$; *rs219780* $r^2 = 0.17$). The association of *rs170183* conditioning on both *rs219779* and *rs219780* remained significant (Stage 1 $P = 3.45 \times 10^{-5}$), implying that *rs170183* may represent a largely independent signal from what was reported previously (22). It is located in an intron of the *CLDN14* (claudin 14) gene (Supplementary Material, Fig. S2), which was previously proposed as a candidate

Table 2. Previous loci replicated in the current study at the GWS level

Region	SNP	Nearby gene	Dis.(kb)	Trait	Stage	N	P-value
1p36.12	rs34920465	ZBTB40	78.0	SPN	1	11 030	**6.01E−10**
					2	8469	5.62E−5
					1 + 2	19 609	**2.67E−13**
1p31.3	rs1430740	GPR177	8.2	SPN	1	11 026	**8.46E−9**
					2	6070	3.50E−4
					1 + 2	17 096	**1.43E−11**
4p16.3	rs6827815	FGFRL1	6.3	FNK	1	11 125	6.01E−7
					2	9161	3.48E−3
					1 + 2	20 286	**9.89E−9**
					3	6663	1.17E−4
					1 + 2 + 3	26 949	**5.19E−12**
4q22.1	rs1463104	MEPE	31.7	SPN	1	11 026	7.08E−7
					2	7303	6.64E−4
					1 + 2	18 329	**2.04E−9**
5q14.3	rs6894139	MEF2C	148.5	FNK	1	11 125	**2.02E−9**
					2	6762	**2.55E−10**
					1 + 2	17 887	**6.86E−18**
6q25.1	rs1871859	C6orf97	0.0	SPN	1	11 029	**1.27E−10**
					2	6070	9.10E−4
					1 + 2	17 099	**9.29E−13**
7q21.3	rs10429035	FLJ42280	0.0	HIP	1	10 444	**4.24E−9**
					2	1882	9.70E−5
					1 + 2	12 326	**4.18E−12**
7q31.31	rs10242100	WNT16	2.2	HIP	1	10 444	**4.63E−8**
					2	2399	8.81E−4
					1 + 2	12 843	**1.94E−10**
8q24.12	rs4424296	TNFRSF11B	48.9	SPN	1	11 029	**5.94E−10**
					2	6070	3.00E−5
					1 + 2	17 099	**8.68E−14**
11p15	rs7108738	SOX6	277.9	FNK	1	11 125	**6.73E−9**
					2	9161	**2.86E−8**
					1 + 2	20 286	**1.03E−15**
11q13.4	rs525592	LRP5	0.0	SPN	1	11 029	9.04E−7
					2	6070	6.74E−6
					1 + 2	17 099	**3.44E−11**
13q14.11	rs9533095	TNFSF11	179.2	SPN	1	11 029	8.32E−8
					2	8469	**2.95E−9**
					1 + 2	19 498	**1.98E−15**
16q24.1	rs71390846	FOXL1	99.4	HIP	1	10 444	**1.29E−9**
					2	1882	0.055
					1 + 2	12 326	**2.36E−10**

gene (22). The product of *CLDN14* is an integral membrane protein and a component of tight junction strands (23). It has been reported to be associated with levels of urinary calcium and serum parathyroid hormone (22), and may therefore regulate bone development through its regulatory effect on calcium metabolism.

The 13 previously reported loci that were replicated in the current study at the GWS level included the following: 1p36.12 (*ZBTB40*), 1p31.3 (*GPR177*), 4p16.3 (*IDUA*, *FGFRL1*), 4q22.1 (*MEPE*), 5q14.3 (*MEF2C*), 6q25.1 (*ESR1*, *C6orf97*), 7q21.3 (*FLJ42280*), 7q31.31 (*WNT16*, *FAM3C*), 8q24.12 (*TNFRSF11B*), 11p15 (*SOX6*), 11q13.4 (*LRP5*), 13q14.11 (*AKAP11*) and 16q24.1 (*FOXL1*) (Table 2). Among these loci, 4p16.3 is of particular interest. *rs6827815* in this loci was strongly associated with FNK-BMD ($P = 5.19 \times 10^{-12}$) and HIP-BMD ($P = 4.38 \times 10^{-9}$). Its association with SPN-BMD was also suggestively significant ($P = 2.44 \times 10^{-4}$). The region was recently reported to be associated with variations in BMD by another SNP (*rs3755955*) (6), which showed association in the current study as well (stage 1 $P =$ 1.80×10^{-6} for FNK-BMD). The signals at both *rs6827815* and *rs3755955* were likely to be derived from the same source due to their strong LD pattern ($r^2 = 0.97$). *rs6827815* is located in the intergenic region between *IDUA* (iduronidase, 1.1 kb) and *FGFRL1* (fibroblast growth factor receptor-like 1, 6.3 kb). Despite being located in the same haplotype block with *IDUA*, *rs6827815* is also in strong LD with multiple SNPs within *FGFRL1* (Supplementary Material, Fig. S3). Even for SNP *rs4647940* in *FGFRL1* that is ∼20.9 kb from *rs6827815*, the LD pattern between these two SNPs remains rather strong ($r^2 = 0.93$). *FGFRL1* is of significant interest due to its biological function. The protein encoded by *FGFRL1*, which is expressed preferentially in skeletal tissues, is a member of the fibroblast growth factor receptor (*FGFR*) family (24). *FGF* and *FGF* receptors have been shown to be important for bone development (25), and mutations in *FGFRL1* induce skeletal disorders in humans (26). *FGFRL1* appears to function as a decoy receptor, i.e. it binds *FGF* ligands, without inducing signal transduction. Thus, the regulatory role of *FGFRL1* is likely to occur through competitive inhibition; it
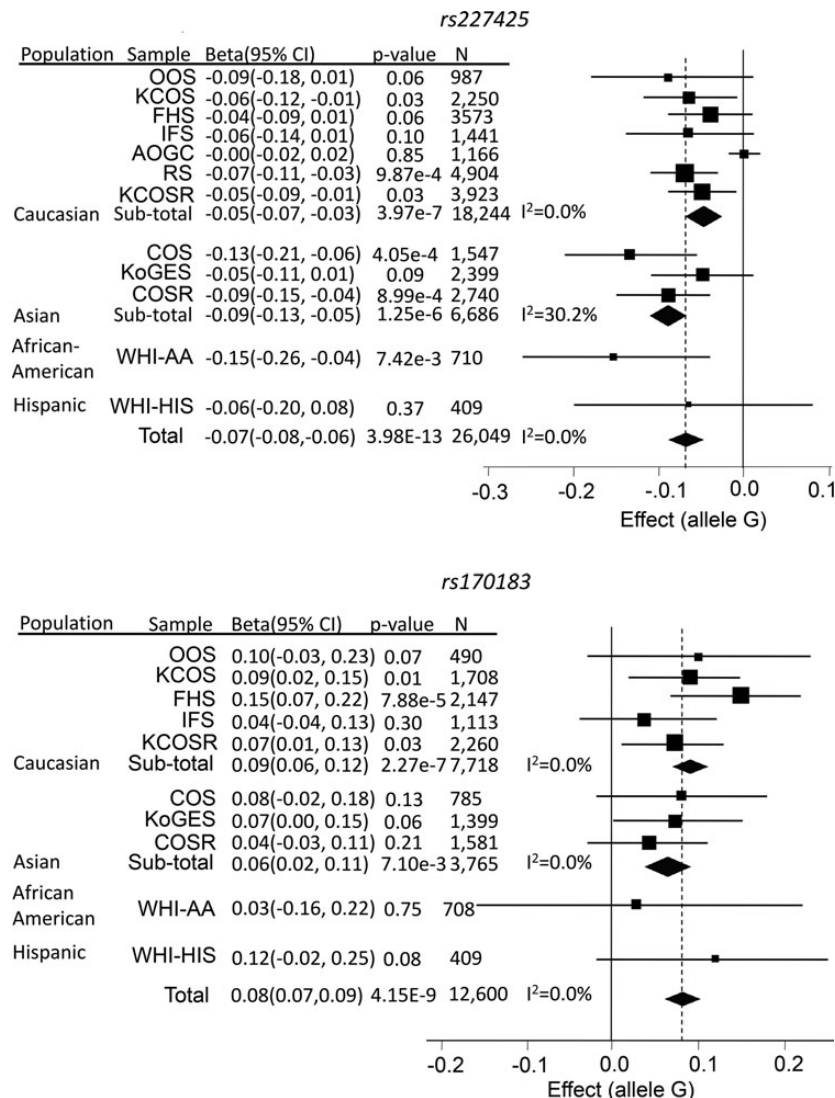
Figure 3. Forest plots for the two newly identified SNPs. Regression coefficient (beta) and its 95% confidence interval (CI) were presented as un-transformed estimates from individual studies.

binds *FGF* ligands and sequesters them away from functional *FGF* receptors (27).

We checked the cumulative effects of identified GWS SNPs on BMD variation in two of the tested samples: KCOS (Kansas City Osteoporosis Study, $n = 2250$) and COS (China Osteoporosis Study, $n = 1547$) samples. Collectively, the two SNPs (*rs227425* and *rs170183*) explained $0.3 - 0.7\%$ of phenotypic variation in BMD. Taking the 13 SNPs from previously reported loci into account, the total explainable phenotypic variation ranged from 2.8 to 4.9% depending on population sample and skeletal site. Considering that heritability of BMD is estimated to be as high as $50-80\%$, the majority of genetic determination for BMD variation still remains to be discovered.

To explore the potential functional relationship between the two candidate genes (*SMOC1* and *CLDN14*) and variations in BMD, we compared their *in vivo* expression in peripheral blood monocytes (PBM; potential osteoclastogenic cells,

which may also secrete cytokines important for bone metabolism) in a group of 15 premenopausal female subjects of Caucasian population with high hip BMD (*z*-score >0.7, 25% top of the phenotypic distribution) versus another group of 14 matched premenopausal female subjects with low hip BMD (*z*-score < -0.5, 30% bottom of the phenotypic distribution). Both genes were differentially expressed in PBMs between the two groups at the nominal level $P < 0.05$ (Table 3), strengthening the argument that these genes may be biologically relevant to the regulation of bone metabolism.

DISCUSSION

In this study, using a three-stage genome-wide association meta-analysis, we have identified two novel loci that are associated with BMD variation at the GWS level. We have also replicated 13 previously identified loci at the GWS level.

Table 3. Gene expressions in PBM cells

Gene	Probe ID	Mean intensity (s.d.)		*P*-value
		High (*n* = 15)	Low (*n* = 14)	
SMOC1	991 408	6.91 (0.72)	6.27 (0.37)	2.93E−3
CLDN14	1 310 762	10.48 (0.64)	10.06 (0.35)	0.04

Gene expressions in human potential osteoclastogenic cells (peripheral blood monocytes, PBMs) were examined. The sample consisted of 29 premenopausal female subjects of European ancestry, 15 of which had high hip BMD (*z*-score >0.7) and 14 had low hip BMD (*z*-score < −0.5). Gene expression experiment was conducted with Affymetrix Human Exon 1.0 ST Array.

Though the samples that we analyzed were diverse in ancestries, neither of the two loci we identified through the present meta-analysis was likely to have emerged from this heterogeneity. First, neither Q nor I^2 measures gave evidence of heterogeneity at either of the identified SNPs. Second, the random-effects model, which is more robust against heterogeneity, gave similar results to the fixed-effects model. Third, sensitivity analysis on the two newly identified SNPs gave consistent results among studies (Supplementary Material, Table S11). Finally, multiple genomic regions that were previously identified using similar analytical approaches were replicated in the present study. Therefore, our newly identified loci are likely to represent true genetic susceptibility loci for variations in BMD that are shared across the different populations studied. Despite lack of validation of the imputation by real genotyping, the two SNPs were accurately imputed with remarkable MACH imputation accuracy measures in Stage 1 (ranging from 0.78 to 0.99). In addition, the real genotyping we performed for all of the >6600 subjects at Stage 3 replication testing showed consistently significant effects for these two SNPs, which partially attests to the high accuracy of the imputation in Stages 1 and 2.

In the recently published paper by the GEFOS (6) a total of 56 SNPs were identified to be associated with SPN and/or FNK-BMDs at the GWS level. Four samples (FHS, RS, IFS and AOGC, *n* = 12 094) used in that study overlapped with the present one. Though both of the newly identified SNPs in the current study were suggestively significant in the overlapped samples (Fig. 3), none of them was significant at the GWS level in the study by Estrada *et al*. (6). Our findings therefore imply that though a new meta-analysis of a smaller sample size is less powerful than that of a larger sample, it may still have power to identify a few novel responsible loci (28,29). For a SNP with an effect as low as 0.05%, the power to detect it is as low as 0.57% (Stage 1 threshold 1×10^{-6}) for a sample of 11 140 subjects. But as we are performing a hypothesis free genome-wide scan, the power to detect at least one of many causal SNPs, i.e. 500, is as high as 94.26%. Nevertheless, for a sample of ∼33 000 discovery subjects, the power to identify/replicate any particular SNP is quite low, only 8.21% at the GWS level, or 24.41% at the suggestive level (GWS threshold 5×10^{-8}, suggestive threshold 1×10^{-6}). Another explanation of our new findings may lie in different heterogeneity settings in different analyses. Of the 56 SNPs identified in Estrada *et al*. (6), 54 were available for analysis in our Stage 1 results (Supplementary Material, Table S12). Among them, 30 were significant after multiple testing adjustment ($P = 0.05/54$). With the random-effects model, however, only 20 of these

30 SNPs retained significance, implicating the potential heterogeneity effects for the remaining 10 SNPs identified earlier in the present study. When extending the analyses to the most significant SNP within the 100 kb flanking region for each reported SNP, 40 were significant with the fixed-effects model, and 35 were significant with the random-effects model (Supplementary Material, Table S12). The non-replicability on the remaining regions implies that heterogeneous effects are sample specific, so that loci identified in one set of samples may be masked in another set of samples due to the specific heterogeneous structures related to that particular set of samples on particular loci.

We recognize that our original discovery sample includes samples that are included in the GEFOS consortium, so the overall evidence of association in the GEFOS paper cannot be taken as completely independent replication. We were unable to obtain results for the subset of GEFOS samples not included in our original discovery sample. We were able to obtain replication data from two samples of the TwinsUK cohort (*n* = 2762 and 1479, respectively) and one sample of the AFOS (*n* = 918/475 combined/female subjects). We therefore removed the GEFOS data from our original discovery data (which still left a genome-wide significant result) and also tried to computationally and theoretically estimate the *P*-values that would have been obtained in the GEFOS data, excluding those samples that are in our discovery set. Nevertheless, independent validation of this finding would be desirable to more completely rule out a false-positive association or to establish population heterogeneity in the genetic effects identified.

On replicating the identified novel SNPs by the GEFOS results, the shift of the overlapped samples from the discovery phase into the replication phase may incur a 'winner's curse' effect (30). Nonetheless, we would expect this effect to have a minimum impact in this case for the following two reasons: first, analysis of samples in the present study without the overlapped samples already achieved (or nearly achieved) the GWS significance level, which means the SNPs could have been selected even without the involvement of any of the GEFOS samples. Second, the most promising and convincing evidence is the combined analysis of all samples, which still leaves the two SNPs significant at the GWS level.

In summary, by performing a multistage genome-wide association meta-analysis, we have identified two novel loci for BMD at the GWS level, and have replicated many previously reported loci. We have also explored the functional importance of the two involved candidate genes by gene expression experiments. Our findings, together with one previously reported larger meta-analysis, provide solid and coincident evidence of association for the two identified loci. The discovery stage GWAS association summary results were available at https://tulane.app.box.com/s/biemkwud7cm3cvn4ut1u.

MATERIALS AND METHODS

Study design

This study of meta-analysis comprises three stages. In Stage 1, we collected seven GWAS samples and performed a meta-analysis of BMDs at the spine, total hip and femoral neck (due to its clinical significance to hip fractures) for association.

In Stage 2, we selected a set of SNPs of interest in Stage 1, and analyzed them *in silico* in three additional samples. Novel SNPs significant, or nearly significant, at the GWS level from joint analysis of both stages were followed up by Stage 3 *de novo* genotyping in two additional samples.

Study populations

This study incorporated samples from multiple research and/or clinical centers. All samples were approved by the respective institutional ethics review boards, and all participants provided written informed consent.

In Stage 1, seven GWAS samples were incorporated, of which three were from in-house studies and four were identified from the database of genotype and phenotype (dbGAP). The three in-house samples consisted of two with 987 (Omaha osteoporosis study, OOS) (5) and 2250 (Kansas City osteoporosis study, KCOS) unrelated individuals, respectively, of European ancestry, and the third (China osteoporosis study, COS) with 1547 unrelated individuals of Chinese Han ancestry. The fourth sample was derived from the Framingham Heart Study (FHS), a longitudinal and prospective cohort comprising >16 000 individuals spanning three generations, of European ancestry (4). Focusing on the first two generations, we identified 3747 phenotyped individuals. The fifth sample was the Indiana Fragility Study (IFS), a cross-sectional cohort comprising 1493 premenopausal sister pairs of European ancestry (6). After quality control, 1488 subjects were qualified for analysis. Both the sixth and seventh samples were derived from the Women's Health Initiative (WHI) observational study, a partial factorial randomized and longitudinal cohort with >12 000 genotyped women aging 50–79 years, of African-American or Hispanic ancestry (31). The sixth sample comprises 712 phenotyped individuals of African-American ancestry, and the seventh sample comprises 409 phenotyped individuals of Hispanic ancestry.

The Stage 2 *in silico* replication incorporated three GWAS samples. The first sample was the RS comprising 4904 unrelated individuals of European ancestry (4). The second sample was the Korean genome epidemiology study (KoGES) comprising 2399 unrelated individuals of Eastern Asian ancestry. The third one was the Anglo-Australasian Osteoporosis Genetics Consortium (AOGC) (10), an extreme-ascertained cohort comprising 1955 unrelated menopausal women of European ancestry with either high total hip BMD (*z*-score between +1.5 and +4.0) or low total hip BMD (*z*-score between −4.0 and −1.5).

The Stage 3 *de novo* genotyping replication included two additional samples, one with 3923 unrelated independent individuals of European ancestry derived from the KCOS (KCOSR) cohort, and the other with 2740 unrelated independent individuals of Chinese Han ancestry derived from the COS (COSR) cohort.

Phenotype measurements and modeling

BMD was measured at the lumbar spine and hip and/or femoral neck with dual-energy X-ray absorptiometry (DXA) scanners (either Lunar Corp., Madison, WI, USA; or Hologic Inc., Bedford, MA, USA was used within individual study samples) following the manufacturer protocols (Supplementary Material,

Table S1). In each of the Stage 1 GWAS samples, covariates were screened among gender, age, age^2, weight, height, scan side (in FHS) and scanner ID (in WHI) with the stepwise linear regression model. Raw BMD measurements were adjusted by significant covariates. To adjust for potential population stratification, the first five principal components derived from genome-wide genotype data were included as covariates (14). Residual phenotypes after adjustment were normalized by inverse quantile of the standard normal distribution to impose a normal distribution on phenotypes that were analyzed subsequently (32).

Genotyping and quality control

All Stage 1 GWAS samples were genotyped by high-throughput SNP genotyping arrays (Affymetrix Inc., Santa Clara, CA, USA; or Illumina Inc., San Diego, CA, USA within individual samples) following the manufacturer's protocols (Supplementary Material, Table S2). Quality control of genotype data were implemented with Plink (18), with the following criteria applied: individual missingness <5%, SNP call rate >95%, and Hardy–Weinberg equilibrium (HWE) *P*-value > 1.0×10^{-5}. For familial samples (FHS and IFS), all genotypes with the Mendel error were set to missing. Population outliers were monitored by principal components derived from genome-wide genotype analysis.

Genotype imputation

Each GWAS sample from Stage 1 was imputed by the 1KG sequence variants (as of August, 2010). Reference haplotypes representing 283 individuals with European ancestry, 193 with Asian ancestry, and 174 with African ancestry were downloaded from MACH (15) download website. Each GWAS sample was imputed by the respective reference panel with the closest ancestry.

Prior to imputation, a consistency test of allele frequency between GWAS and reference samples was examined with the chi-square test. To correct for potential mis-strandedness, GWAS SNPs that failed a consistency test ($P < 1.0 \times 10^{-6}$) were transformed into reverse strand. SNPs that again failed consistency were removed from the GWAS sample.

To distribute imputation computation to multiple parallel CPUs, chromosomes were split into non-overlapping fragments each of 10 Mb length. In each fragment, haplotypes of individual GWAS were phased by a Markov Chain Haplotyping algorithm (MACH) (15). For familial samples (FHS and IFS), 200 unrelated founder individuals were randomly selected to estimate model parameters, which were then used to impute all family members. Based on phased haplotypes, untyped genotypes were then imputed by a computationally efficient imputing algorithm Minimac (15). Each GWAS sample was imputed by relevant population's reference haplotypes. SNPs with r^2 score <0.3 as estimated by Minimac were considered of poor imputation accuracy. SNPs of high accuracy in at least two samples, and of minor allele frequency (MAF) >0.05 in at least one sample, were included for subsequent analyses.

Stage 1 association testing

Each GWAS sample was tested for association between phenotypes and genotyped and imputed SNPs under an additive mode

of inheritance. For unrelated samples, association was examined by the linear regression model with MACH2QTL (15), in which allele dosage was taken as the predictor for the phenotype. For familial samples (FHS and IFS), a mixed linear model was used in which the effect of genetic relatedness within each pedigree was also taken into account (16). Genomic control inflation factor (33) was estimated for each individual GWAS. Associations in both the gender combined sample and gender-specific samples were examined.

Stage 1 meta-analysis

Summary statistics of associations from each GWAS were combined to perform weighted fixed-effect meta-analysis with METAL (34), in which weights were proportional to the square-root of each sample size. *Cochran*'s Q statistic and I^2 were calculated as measures of between-study heterogeneity (35). Random-effect meta-analyses were performed to those SNPs with Q P-value of <0.05 or I^2 value $>50\%$ with the standard procedure *meta.summaries* in the R package *rmeta*.

Stage *2 in silico* analysis

A total of 33 SNPs, each representing a distinct genomic region, were selected for Stage 2 *in silico* analyses. The prioritization of SNPs for Stage 2 was primarily based on the strongest P-values, with a few exceptions in which the consistency of direction of the effects was also considered. PCA was applied in all Stage 2 samples to account for population stratification effects. For imputation, the RS used overlapping fragments each of 2000 markers with 100 markers of overlap to improve imputation quality. Overlapping regions were removed after imputation. Association analyses in the RS sample were performed with MACH2QTL (15) via GRIMP (36) (which uses genotype dosage value as a predictor in a linear regression framework). Imputation and association analyses in KoGES were performed with IMPUTE2 (37) and Plink (18). For the AOGC sample, genotypes data quality control was performed as in the earlier study (10). Effective BMD was calculated correcting for weight, age, age^2 and the first four eigenvectors of the principle components (14). The 16 densitometers for BMD measurement were taken as random variables to adjust for their effects. Imputation was performed with MACH (15), with the 1KG European reference panel (as of August 2010). The corrected BMD distribution follows an approximate normal distribution using the Shapiro–Wilk normality test ($P = 0.537$). MACH2QTL (15) was used to perform the association analysis. The summary statistics of Stage 2 were meta-analyzed with Stage 1 results with METAL (34).

Stage 3 *de novo* genotyping analysis

Joint analyses of Stages 1 and 2 produced at GWS level 12 loci that had been reported previously, and 3 new loci (one was reported during the preparation of this manuscript). The three SNPs were followed up in Stage 3 of *de novo* genotyping in two independent samples, namely KCOSR and COSR. The KCOSR and COSR samples were genotyped by Kbiosciences (UK) and Shanghai Biowing (China) companies, respectively. Quality control included individual missingness $<5\%$, SNP call rate $>90\%$, and HWE P-value $>1.0 \times 10^{-5}$. Associations

for Stage 3 were examined with Plink (18). Joint meta-analysis of Stage $1 + 2 + 3$ were performed with METAL (34), and regional Manhattan plot was drawn with LocusZoom (38).

Sensitivity analysis

Sensitivity analyses were conducted by removing each study in turn, studies with Asian ancestry, and studies with African and Hispanics ancestries, respectively.

Gene expression analysis in human osteoclasts

The two candidate genes (*SMOC1* and *CLDN14*) implied by the identified SNPs were tested for their expressions in human potential osteoclastogenic cells (PBMs) between subjects with high versus low BMDs. The sample consisted of 29 premenopausal female subjects of European ancestry, 15 of which were with high hip BMD (z-score >0.7, 25% top of the phenotypic distribution) and 14 were with low hip BMD (z-score <-0.5, 30% bottom of the phenotypic distribution). Gene expression experiment was a part of an ongoing project, conducted with Affymetrix Human Exon 1.0 ST Array following the manufacturer protocols. Association analyses of gene expression intensities between the two groups were performed with the R package *linear models for microarray data* (*limma*) (39).

SUPPLEMENTARY MATERIAL

Supplementary Material is available at *HMG* online.

ACKNOWLEDGEMENTS

REFERENCES

1. Cummings, S.R. and Melton, L.J. (2002) Epidemiology and outcomes of osteoporotic fractures. *Lancet*, **359**, 1761–1767.
2. Reginster, J.Y. and Burlet, N. (2006) Osteoporosis: a still increasing prevalence. *Bone*, **38**, S4–S9.
3. Peacock, M., Turner, C.H., Econs, M.J. and Foroud, T. (2002) Genetics of osteoporosis. *Endocr. Rev.*, **23**, 303–326.
4. Rivadeneira, F., Styrkarsdottir, U., Estrada, K., Halldorsson, B.V., Hsu, Y.H., Richards, J.B., Zillikens, M.C., Kavvoura, F.K., Amin, N., Aulchenko, Y.S. *et al.* (2009) Twenty bone-mineral-density loci identified by large-scale meta-analysis of genome-wide association studies. *Nat. Genet.*, **41**, 1199–1206.
5. Xiong, D.H., Liu, X.G., Guo, Y.F., Tan, L.J., Wang, L., Sha, B.Y., Tang, Z.H., Pan, F., Yang, T.L., Chen, X.D. *et al.* (2009) Genome-wide association

and follow-up replication studies identified ADAMTS18 and TGFBR3 as bone mass candidate genes in different ethnic groups. *Am. J. Hum. Genet.*, **84**, 388–398.

6. Estrada, K., Styrkarsdottir, U., Evangelou, E., Hsu, Y.H., Duncan, E.L., Ntzani, E.E., Oei, L., Albagha, O.M., Amin, N., Kemp, J.P. *et al.* (2012) Genome-wide meta-analysis identifies 56 bone mineral density loci and reveals 14 loci associated with risk of fracture. *Nat. Genet.*, **44**, 491–501.

7. Richards, J.B., Rivadeneira, F., Inouye, M., Pastinen, T.M., Soranzo, N., Wilson, S.G., Andrew, T., Falchi, M., Gwilliam, R., Ahmadi, K.R. *et al.* (2008) Bone mineral density, osteoporosis, and osteoporotic fractures: a genome-wide association study. *Lancet*, **371**, 1505–1512.

8. Styrkarsdottir, U., Halldorsson, B.V., Gretarsdottir, S., Gudbjartsson, D.F., Walters, G.B., Ingvarsson, T., Jonsdottir, T., Saemundsdottir, J., Center, J.R., Nguyen, T.V. *et al.* (2008) Multiple genetic loci for bone mineral density and fractures. *N. Engl. J. Med.*, **358**, 2355–2365.

9. Styrkarsdottir, U., Halldorsson, B.V., Gretarsdottir, S., Gudbjartsson, D.F., Walters, G.B., Ingvarsson, T., Jonsdottir, T., Saemundsdottir, J., Snorradottir, S., Center, J.R. *et al.* (2009) New sequence variants associated with bone mineral density. *Nat. Genet.*, **41**, 15–17.

10. Duncan, E.L., Danoy, P., Kemp, J.P., Leo, P.J., McCloskey, E., Nicholson, G.C., Eastell, R., Prince, R.L., Eisman, J.A., Jones, G. *et al.* (2011) Genome-wide association study using extreme truncate selection identifies novel genes affecting bone mineral density and fracture risk. *PLoS. Genet.*, **7**, e1001372.

11. Duan, Q., Liu, E.Y., Croteau-Chonka, D.C., Mohlke, K.L. and Li, Y. (2013) A comprehensive SNP and indel imputability database. *Bioinformatics*, **29**, 528–531.

12. Guo, Y., Tan, L.J., Lei, S.F., Yang, T.L., Chen, X.D., Zhang, F., Chen, Y., Pan, F., Yan, H., Liu, X. *et al.* (2010) Genome-wide association study identifies ALDH7A1 as a novel susceptibility gene for osteoporosis. *PLoS Genet.*, **6**, e1000806.

13. The 1000 Genomes Project Consortium. (2011) A map of human genome variation from population-scale sequencing. *Nature*, **467**, 1061–1073.

14. Pasaniuc, B., Zaitlen, N., Bhatia, G., Gusev, A., Patterson, N. and Price, A. (2012) Fast and accurate 1000 Genomes imputation using summary statistics or low-coverage sequencing data. (Program #89). Presented at the 62nd Annual Meeting of The American Society of Human Genetics, November 8, 2012 in San Francisco, California.

15. Li, Y., Willer, C.J., Ding, J., Scheet, P. and Abecasis, G.R. (2010) MaCH: using sequence and genotype data to estimate haplotypes and unobserved genotypes. *Genet. Epidemiol.*, **34**, 816–834.

16. Zhang, L., Li, J., Pei, Y.F., Liu, Y. and Deng, H.W. (2009) Tests of association for quantitative traits in nuclear families using principal components to correct for population stratification. *Ann. Hum. Genet.*, **73**, 601–613.

17. Chi, E.C., Zhou, H., Chen, G.K., Ortega Del Vecchyo, D. and Lange, K.L. (2013) Genotype imputation via matrix completion. *Genome Res.*, **23**, 509–518.

18. Purcell, S., Neale, B., Todd-Brown, K., Thomas, L., Ferreira, M.A., Bender, D., Maller, J., Sklar, P., de Bakker, P.I., Daly, M.J. *et al.* (2007) PLINK: a tool set for whole-genome association and population-based linkage analyses. *Am. J. Hum. Genet.*, **81**, 559–575.

19. Vannahme, C., Smyth, N., Miosge, N., Gosling, S., Frie, C., Paulsson, M., Maurer, P. and Hartmann, U. (2002) Characterization of SMOC-1, a novel modular calcium-binding protein in basement membranes. *J. Biol. Chem.*, **277**, 37977–37986.

20. Choi, Y.A., Lim, J., Kim, K.M., Acharya, B., Cho, J.Y., Bae, Y.C., Shin, H.I., Kim, S.Y. and Park, E.K. (2010) Secretome analysis of human BMSCs and identification of SMOC1 as an important ECM protein in osteoblast differentiation. *J. Proteome Res.*, **9**, 2946–2956.

21. Okada, I., Hamanoue, H., Terada, K., Tohma, T., Megarbane, A., Chouery, E., Abou-Ghoch, J., Jalkh, N., Cogulu, O., Ozkinay, F. *et al.* (2011) SMOC1 is essential for ocular and limb development in humans and mice. *Am. J. Hum. Genet.*, **88**, 30–41.

22. Thorleifsson, G., Holm, H., Edvardsson, V., Walters, G.B., Styrkarsdottir, U., Gudbjartsson, D.F., Sulem, P., Halldorsson, B.V., de Vegt, F., d'Ancona, F.C. *et al.* (2009) Sequence variants in the CLDN14 gene associate with kidney stones and bone mineral density. *Nat. Genet.*, **41**, 926–930.

23. Lal-Nag, M. and Morin, P.J. (2009) The claudins. *Genome. Biol.*, **10**, 235.

24. Trueb, B., Zhuang, L., Taeschler, S. and Wiedemann, M. (2003) Characterization of FGFRL1, a novel fibroblast growth factor (FGF) receptor preferentially expressed in skeletal tissues. *J. Biol. Chem.*, **278**, 33857–33865.

25. Sahni, M., Ambrosetti, D.C., Mansukhani, A., Gertner, R., Levy, D. and Basilico, C. (1999) FGF signaling inhibits chondrocyte proliferation and regulates bone development through the STAT-1 pathway. *Genes. Dev.*, **13**, 1361–1366.

26. Rieckmann, T., Zhuang, L., Fluck, C.E. and Trueb, B. (2009) Characterization of the first FGFRL1 mutation identified in a craniosynostosis patient. *Biochim. Biophys. Acta*, **1792**, 112–121.

27. Steinberg, F., Zhuang, L., Beyeler, M., Kalin, R.E., Mullis, P.E., Brandli, A.W. and Trueb, B. (2010) The FGFRL1 receptor is shed from cell membranes, binds fibroblast growth factors (FGFs), and antagonizes FGF signaling in Xenopus embryos. *J. Biol. Chem.*, **285**, 2193–2202.

28. Liu, Y.J., Zhang, L., Pei, Y., Papasian, C.J. and Deng, H.W. (2013) On genome-wide association studies and their meta-analyses: lessons learned from osteoporosis studies. *J. Clin. Endocrinol. Metab.*, **98**, E1278–E1282.

29. Pei, Y.F., Zhang, L., Papasian, C.J., Wang, Y.P. and Deng, H.W. (2013) On individual genome-wide association studies and their meta-analysis. *Hum. Genet.*, doi: 10.1007/s00439-013-1366-4.

30. Thaler, R.H. (1988) Anomalies: the winner's curse. *J. Econ. Perspect.*, **2**, 191–202.

31. The Women's Health Initiative Study Group. (1998) Design of the Women's Health Initiative clinical trial and observational study. The Women's Health Initiative Study Group. *Control. Clin. Trials*, **19**, 61–109.

32. Peng, B., Yu, R.K., Dehoff, K.L. and Amos, C.I. (2007) Normalizing a large number of quantitative traits using empirical normal quantile transformation. *BMC Proc.*, **1**(Suppl. 1), S156.

33. Devlin, B. and Roeder, K. (1999) Genomic control for association studies. *Biometrics*, **55**, 997–1004.

34. Willer, C.J., Li, Y. and Abecasis, G.R. (2010) METAL: fast and efficient meta-analysis of genomewide association scans. *Bioinformatics*, **26**, 2190–2191.

35. Higgins, J.P., Thompson, S.G., Deeks, J.J. and Altman, D.G. (2003) Measuring inconsistency in meta-analyses. *BMJ*, **327**, 557–560.

36. Estrada, K., Abuseiris, A., Grosveld, F.G., Uitterlinden, A.G., Knoch, T.A. and Rivadeneira, F. (2009) GRIMP: a web- and grid-based tool for high-speed analysis of large-scale genome-wide association using imputed data. *Bioinformatics*, **25**, 2750–2752.

37. Howie, B.N., Donnelly, P. and Marchini, J. (2009) A flexible and accurate genotype imputation method for the next generation of genome-wide association studies. *PLoS Genet.*, **5**, e1000529.

38. Pruim, R.J., Welch, R.P., Sanna, S., Teslovich, T.M., Chines, P.S., Gliedt, T.P., Boehnke, M., Abecasis, G.R. and Willer, C.J. (2010) LocusZoom: regional visualization of genome-wide association scan results. *Bioinformatics*, **26**, 2336–2337.

39. Smyth, G.K. (2004) Linear models and empirical bayes methods for assessing differential expression in microarray experiments. *Stat. Appl. Genet. Mol. Biol.*, **3**, Article3.